

Small-Angle Neutron Scattering Determination of Macrolattice Structure in a Polystyrene-Polybutadiene Diblock Copolymer

F. S. Bates and R. E. Cohen*

Department of Chemical Engineering, Massachusetts Institute of Technology, Cambridge, Massachusetts 02139

C. V. Berney

Department of Nuclear Engineering, Massachusetts Institute of Technology, Cambridge, Massachusetts 02139. Received July 20, 1981

ABSTRACT: A polystyrene-polybutadiene diblock copolymer (in which the butadiene phase is deuterated to enhance neutron contrast) has been synthesized and its morphology (polybutadiene spheres in a polystyrene matrix) determined by electron microscopy. Small-angle neutron scattering experiments give well-resolved Bragg peaks whose positions show that the packing of the polybutadiene spheres is either simple cubic or body-centered cubic. The scattering data give a mean radius of 124 Å for the polybutadiene spheres; this result (together with unit cell dimensions from the Bragg peaks) allows calculations of an estimated volume fraction of polybutadiene for each packing mode. Comparison with an experimentally derived value indicates that the packing is body-centered cubic.

Introduction

Microphase separation in block copolymers is a well-documented phenomenon that has been addressed in numerous experimental and theoretical investigations. The spherical, cylindrical, and lamellar microdomain morphologies have been used to advantage in commercial applications and in the construction of model materials for research. Within this broad field some important unanswered questions remain to be resolved. One of these relates to the spherical morphology of block copolymers. In the construction of his theory of microphase separation of block copolymers, Helfand¹ has assumed a close-packed arrangement for the spherical morphology. On the other hand, the recent theoretical work of Leibler² indicates that a body-centered cubic lattice of spheres (not a close-packed arrangement) is the most stable morphology. Detailed experimental evidence that would assist in the resolution of this question is scarce and somewhat conflicting. Using combined evidence from electron microscopy and from "ping-pong ball" models, Pedemonte et al.³ were able to infer that spherical domains in extruded plugs of a commercial polystyrene-polybutadiene-polystyrene (SBS) triblock copolymer were arranged in a body-centered cubic lattice. Gallot⁴ has also proposed that a body-centered cubic arrangement of spheres is consistent with his experimental evidence. The recent small-angle X-ray scattering (SAXS) experiments of Hashimoto et al.,⁵ carried out on a series of polystyrene-polyisoprene (SI) diblocks, revealed a cubic lattice of spherical domains in all cases; a simple cubic or a somewhat distorted cubic close-packed arrangement was suggested by these authors. Roe and Fishkis⁶ carried out SAXS experiments on SB and SBS block copolymers and tentatively concluded that the morphology of their samples had either a face-centered cubic or a body-centered cubic arrangement of spherical domains. Finally, Richards and Thomason⁷ examined various SI, SIS, and perdeuterated polystyrene-polyisoprene block copolymers by electron microscopy, by SAXS, and by small-angle neutron scattering (SANS). From their data Richards and Thomason proposed that a face-centered cubic arrangement of spheres existed in their samples.

In the present paper we report the results of some of our recent SANS experiments carried out at the National Center for Small-Angle Scattering Research at the Oak Ridge National Laboratory. As part of a larger study

designed to examine relationships between the microphase-separated morphologies, interfacial structure, and mechanical behavior of block copolymers and polymer blends, we have carried out extensive SANS experiments on several polystyrene-perdeuterated polybutadiene (SB_d) diblock copolymers that were synthesized in our laboratory. Deuterated butadiene was used in order to enhance the contrast (for neutron scattering) between the microphase domains. Results obtained on one of these samples are presented in detail in the present paper. A more complete description of the data obtained on our full set of samples will be presented elsewhere. The results presented here, however, shed considerable light on the particular question of the packing arrangement of spherical domains in microphase-separated block copolymers.

Experimental Section

Materials. Styrene monomer (Aldrich Chemical Co.) was deinhhibited by washing with 10% NaOH followed by distilled water and was stored over CaH₂ at 0 °C. Prior to use, the styrene was distilled and redistilled from fresh Na wire and used within 2 h.

1,3-Butadiene (Matheson) was deinhhibited with a 10% NaOH solution, dried over NaOH pellets and molecular sieves, and stirred over CaH₂ at 0 °C for 24 h. The butadiene was then condensed over several Na mirrors and was frozen until used.

1,3-Butadiene-*d*₆ (Merck, Sharp and Dohme, Ltd.) was stirred over CaH₂ at 0 °C for 24 h, condensed over several Na mirrors, and frozen until used. The reported 98 atom % deuterium was verified by mass spectrometry.

n-Butyllithium (Aldrich) was diluted with cyclohexane and titrated by the method of Eppley and Dixon.⁸ Reagent grade benzene (J. T. Baker Co.) was distilled twice under argon; a small amount of anisole was added⁹ and this mixture was purified by a previously reported "living gel" technique.¹⁰ Reagent grade toluene was used as received from J. T. Baker Co.

Synthesis. Polymerizations were carried out under highly purified argon in a Pyrex reactor fitted with Teflon connectors. Benzene initiator and styrene were added to the reactor and vigorously stirred for several hours at 40 °C. Following removal of a small sample for later analysis, the butadiene was introduced to the reactor and the temperature was raised to 50 °C. After several hours the reaction was terminated with methanol. The polymer was precipitated with methanol, dried under vacuum for several days, and stored at -20 °C.

Molecular Characterization. Two well-matched block copolymers (one containing perdeuterated polybutadiene) and their corresponding polystyrene blocks were analyzed by high-pressure size exclusion chromatography (HPSEC) employing a set of

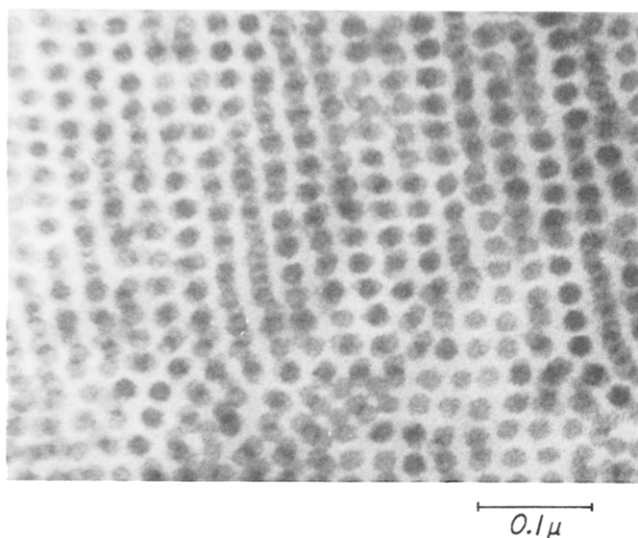


Figure 1. Transmission electron micrograph of a thin section of sample SB_d-1 stained with osmium tetroxide. Darkened polybutadiene spheres have an estimated characteristic radius of 94 Å.

Table I
Molecular Characterization

sample	$10^{-3}M_n^S$	$(M_w/M_n)^S$	$10^{-3}M_n^{SB}$	$(M_w/M_n)^{SB}$
SB-1	79 ^a	1.06 ^a	90 ^b	1.06 ^a
SB _d -1	80 ^a	1.06 ^a	93 ^b	1.07 ^a
	92 ^c		106 ^d	

^a HPSEC. ^b Using M_n^S and UV absorption data.

^c Using osmometry data and UV absorption data.

^d Osmometry.

Zorbax PSM bimodal columns, with toluene as the mobile phase. The HPSEC experiments were calibrated with 10 polystyrene standards. Diblock copolymer compositions were determined by UV absorption in chloroform at a wavelength of 262 nm; the weight fraction of perdeuterated polybutadiene thus obtained was 0.136, a figure which agrees with the synthesis stoichiometry. The molecular weight of the diblock containing perdeuterated polybutadiene was determined by membrane osmometry. Characterization results are summarized in Table I. Results from all methods are in approximate agreement with a molecular weight of 80 000 for the polystyrene and 13 000 for the polybutadiene fraction. The microstructure of the hydrogenated polybutadiene was determined by proton NMR to be 87% mixed cis and trans 1,4 and 13% 1,2 addition; the perdeuterated polybutadiene microstructure is assumed to be essentially identical.

Structural Analysis. Samples were prepared by a spin-casting technique,¹¹ starting with 5% solutions of the copolymer in toluene. Solvent was removed at 80 °C over a period of several days while a nitrogen atmosphere was maintained around the entire apparatus. Uniform thin films (approximately 0.5 mm) were obtained in this way. Samples were then annealed under vacuum for 24 h at 120 °C, slowly cooled to room temperature, and stored in the dark under vacuum.

Electron micrographs were obtained on a Philips 200 electron microscope operating at 80 kV and calibrated against a diffraction grating carbon replica (21 600 lines/cm). Samples were stained with osmium tetroxide¹² and sectioned on an LKB ultramicrotome fitted with a diamond knife.

Small-angle neutron scattering patterns were obtained on the 30-m instrument at the National Center for Small-Angle Research, Oak Ridge National Laboratory. Best results were obtained with a four-layer specimen of 2-mm thickness. Neutrons of 4.75-Å wavelength were used. The scattering curves presented here have been corrected for background scattering and detector sensitivity.

Results and Discussion

Figure 1 is an electron micrograph of sample SB_d-1. The micrograph confirms that the morphology corresponds to

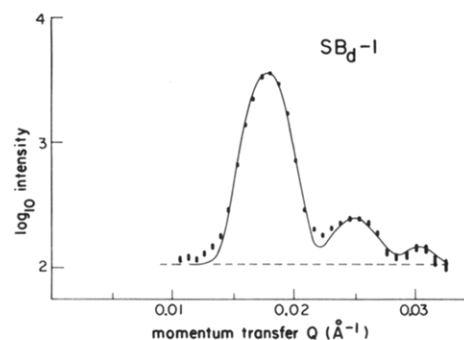


Figure 2. SANS spectrum of sample SB_d-1 at a sample-detector distance L of 15.3 m (source pinhole = 1.0-cm diameter, sample pinhole = 0.6-cm diameter, run time = 1 h). The data points are generated by radially averaging counts accumulated on a two-dimensional detector. The solid curve represents the summed contributions of a set of Gaussian functions fit to the data.

spherical domains of polybutadiene in a matrix of polystyrene and provides an estimated radius of 94 Å for the spheres. It also gives immediate evidence of regularity in the arrangement of the domains, which form a structure sometimes referred to as a paracrystalline macrolattice.¹³ The pattern observed suggests some sort of cubic arrangement, but without three-dimensional information it is impossible to draw a definite conclusion.

We have obtained information on the structure of the macrolattice by means of the small-angle neutron scattering experiments mentioned above. The use of deuterated butadiene resulted in a sample that scattered strongly, allowing observation of details that were absent or unclear in parallel experiments carried out on the undeuterated sample.

Scattering patterns were obtained with the neutron detector set at distances of 15.3, 7.0, 4.2, and 1.8 m from the sample. At the longer distances, resolution is maximized, but the range of momentum transfer Q is reduced ($Q = 4\pi\lambda^{-1}\sin\theta$, where λ is the neutron wavelength of 4.75 Å and θ is half the scattering angle). The 15.3-m data exhibit three well-resolved peaks; we interpret these as being due to Bragg scattering from the macrolattice (that is, we are in fact observing a Debye-Scherrer powder pattern). Figure 2 shows these peaks together with a calculated curve consisting of three Gaussian functions

$$c_i \exp \left[-\frac{1}{2} \left(\frac{Q - q_i}{\sigma_i} \right)^2 \right]$$

added to an arbitrary background. Values for the peak positions q_i obtained from this simulation are 0.0181 Å⁻¹ for the main peak and 0.0255 and 0.031 Å⁻¹ for the subsidiary peaks (width parameters σ_i are 0.0013, 0.0016, and 0.0010 Å⁻¹).

It is well-known¹⁴ that packing arrangements can theoretically be distinguished by the relative positions of the observed Bragg peaks. Table II shows the predicted peak positions q_i of the two subsidiary peaks for four simple packing modes. We have essentially exact agreement for two cases: body-centered cubic (bcc) and simple cubic. In the case of simple cubic packing, the main peak is the (100) reflection, and the edge of the unit cell is $a = 2\pi/0.0181 = 347$ Å. If the packing is bcc, the first allowed reflection is the (110) peak, and $a = (\sqrt{2})347 = 491$ Å.

Figure 3 is a composite of scattering patterns obtained with the detector set at all the distances mentioned above; the data thus cover a much wider range of Q than in Figure 2. It is theoretically possible to distinguish between simple cubic and bcc packing at higher Q since the (321) reflection

Table II
Predicted Bragg Peaks for Simple Packing Arrangements

	allowed peaks (hkl)	relative Q	predicted q_i
bcc	(110)	(1)	(0.0181)
	(200)	1.414	0.0255
	(211)	1.732	0.0313
simple cubic	(100)	(1)	(0.0181)
	(110)	1.414	0.0255
	(111)	1.732	0.0313
fcc	(111)	(1)	(0.0181)
	(200)	1.155	0.0208
	(220)	1.632	0.0295
hcp ($c/a = 1.633$)	(001)	(1)	(0.0181)
	(100)	1.886	0.0340
	(002)	2	0.0361

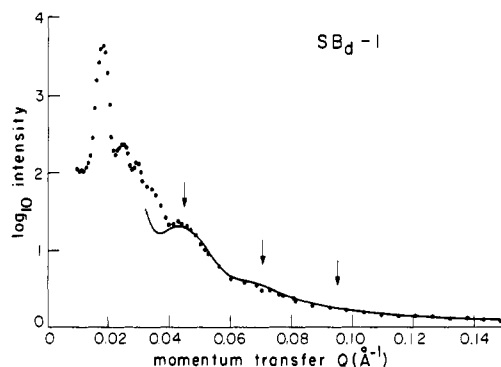


Figure 3. Composite SANS spectrum of sample SB_d-1 including data taken with $L = 15.3, 7.0, 4.2$, and 1.8 m. The solid curve is the calculated intraparticle scattering for a system of spheres of mean radius $R = 124$ Å, radial dispersion $\sigma_R = 15$ Å, and an interfacial thickness of 20 Å. The arrows indicate the positions of Bessel function maxima ($QR = 5.765, 9.10, 12.33$) for $R = 124$ Å. The mismatch below $Q \approx 0.04$ Å⁻¹ is due to interparticle (Bragg) scattering, which was not included in the calculation.

in bcc materials gives rise to a peak at $\sqrt{7}$ times the Q of the main peak (at 0.048 Å⁻¹ in the present case), while there is a gap between the $\sqrt{6}$ and $\sqrt{8}$ positions for a simple cubic lattice. However, this possible gap occurs in a region where intraparticle scattering (rather than Bragg scattering) is the dominant mechanism, thus vitiating its usefulness for distinguishing between simple cubic and bcc packing.

Intraparticle scattering from a collection of uniform spheres of radius R can be described¹⁵ by a form factor

$$\langle f(Q) \rangle^2 = \frac{9\pi}{2} [J_{3/2}(QR) / (QR)^{3/2}]^2$$

The Bessel function $J_{3/2}$ is periodic, producing local maxima at $QR = 5.765, 9.10, 12.33$, etc. We assign the broad feature around 0.045 Å⁻¹ (Figure 3) as the first of these maxima, obtaining a value of 128 Å for R . In order to determine R with greater confidence and precision, we have calculated the intraparticle scattering using a formalism that includes the effect of variation in sphere size⁵ and interfacial thickness.¹⁶ Agreement with the observed scattering data is obtained only within fairly narrow limits for these parameters; the solid curve in Figure 3 shows the best fit, obtained with $R = 124 \pm 3$ Å, σ_R (standard deviation of sphere size) = 15 ± 2 Å, and ΔR (interfacial thickness) = 20 ± 2 Å ($\Delta R = (2\pi)^{1/2}\sigma$, where σ is the standard deviation of a Gaussian smoothing function). The value of R thus obtained is about 30% higher than the estimate from the electron micrographs. A similar

discrepancy between electron microscopy and small-angle X-ray scattering results in lamellar polypropylene has been reported by Stribeck.¹⁷ Sample preparation for electron microscopy involves sectioning and staining, and the effects of the latter process on apparent image size have not been thoroughly studied. Since the SANS experiment is carried out on an unperturbed sample of macroscopic dimensions and since sphere size determination from the neutron scattering curve is relatively direct and unambiguous, we accept the SANS value of $R = 124$ Å and regard the smaller value obtained on the electron microscope as an artifact. We will discuss this inconsistency more thoroughly in a future report.

With R thus determined, it is possible to calculate an estimated volume fraction of polybutadiene V_B for the possible packing modes simple cubic ($a = 347$ Å, $n = 1$ sphere per unit cell) and bcc ($a = 491$ Å, $n = 2$):

$$V_B^{\text{calc}} = n(4/3)\pi R^3/a^3$$

The result for a simple cubic lattice is 0.191 ± 0.015 ; for bcc it is 0.135 ± 0.011 . The observed weight fraction of deuterated polybutadiene, 0.136 , can be converted into an estimated volume fraction; assuming densities of 1.05 for polystyrene¹⁸ and 0.99 for deuterated polybutadiene, the result is 0.142 . Thus the bcc packing mode is definitely established.

Our findings make contact with theoretical predictions in two areas: (a) verification of bcc packing confirms Leibler's prediction,² and (b) our estimated radius of 124 Å is only 9% lower than the value of 137 Å predicted by Helfand's theory.¹ Of the three domain types described by various equilibrium theories of microphase separation, the spherical morphology is the one most likely to exist in actual samples in a kinetically "locked" nonequilibrium condition. The relatively close agreement noted above suggests that the comparatively low molecular weight of sample SB_d-1 led to a close-to-equilibrium structure at the onset of microphase separation. A similar sample of higher molecular weight ($M_w^S = 380\,000$; $M_w^B = 46\,000$) exhibited much less long-range order in electron micrographs and SANS spectra and gave sphere sizes that were markedly smaller than predictions from Helfand's equilibrium theory. A detailed discussion of these results will appear in a forthcoming publication.

Acknowledgment. This research was supported by the National Science Foundation, Division of Materials Research—Polymers Program, under Grants No. DMR-8001674 and DMR-7824185. SANS experiments were performed at the National Center for Small-Angle Scattering Research (NCSASR), which is funded by NSF Grant No. DMR-77-244-58 through interagency agreement No. 40-637-77 with DOE. The center is operated by Union Carbide Corp. under DOE Contract No. W-7405-eng-26. The assistance of Dr. George Wignall of NCSASR is gratefully acknowledged.

References and Notes

- (1) Helfand, E.; Wasserman, Z. R. *Macromolecules* **1978**, *11*, 960.
- (2) Leibler, L. *Macromolecules* **1980**, *13*, 1602.
- (3) Pedemonte, E.; Turturro, A.; Bianchi, V.; Devetta, P. *Polymer* **1973**, *14*, 145.
- (4) Douy, A.; Gallot, B. *Makromol. Chem.* **1981**, *182*, 265.
- (5) Hashimoto, T.; Fujimura, M.; Kawai, H. *Macromolecules* **1980**, *13*, 1660.
- (6) Roe, R.-J.; Fishkis, M.; Chang, J. C. *Macromolecules* **1981**, *14*, 1091.
- (7) Richards, R. W.; Thomason, J. L. *Polymer* **1981**, *22*, 581.
- (8) Eppley, R. L.; Dixon, J. A. *J. Organomet. Chem.* **1967**, *8*, 176.
- (9) Geerts, J.; Van Beylen, M.; Smets, G. *J. Polym. Sci., Part A-1* **1969**, *7*, 2805.

- (10) Bates, F. S.; Cohen, R. E. *Macromolecules* 1981, 14, 881.
- (11) Ramos, A. R.; Cohen, R. E. *Polym. Eng. Sci.* 1977, 17, 639.
- (12) Kato, K. *J. Polym. Sci., Polym. Lett. Ed.* 1966, 4, 35.
- (13) Hosemann, R.; Bagchi, S. N. "Direct Analysis of Matter by Diffraction"; North-Holland Publishing Co.: Amsterdam, 1962.
- (14) Cohen, J. B. "Diffraction Methods in Materials Science"; Macmillan: New York, 1966.
- (15) Guinier, A.; Fournet, G. "Small-Angle Scattering of X-Rays"; Wiley: New York, 1955.
- (16) Koberstein, J. T.; Morra, B.; Stein, R. S. *J. Appl. Crystallogr.* 1980, 13, 34.
- (17) Stribeck, N. Ph.D. Dissertation, Philipps-Universität, Marburg/Lahn, 1980.
- (18) Brandrup, J.; Immergut, E. H., Eds. "Polymer Handbook", 2nd ed.; Wiley: New York, 1975.

Electrohydrodynamic Instabilities in the Nematic Phase of a Homopolyester from 4,4'-Dihydroxy- α -methylstilbene

William R. Krigbaum,* Clara E. Grantham, and Hiro Toriumi

Department of Chemistry, Gross Chemical Laboratory, Duke University, Durham, North Carolina 27706. Received August 13, 1981

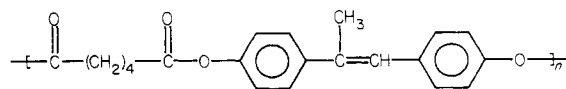
ABSTRACT: Electric field induced flow instabilities are examined for a nematogenic homopolyester of low molecular weight, P-6, synthesized from 4,4'-dihydroxy- α -methylstilbene and adipic acid. The observations for P-6 are compared with the behavior of the low molecular weight nematogen (*p*-methoxybenzylidene)-*p*-*n*-butylaniline (MBBA) and with those reported previously for a high molecular weight nematogenic copolyester, T2/60. In the conduction regime, P-6 forms a fluctuating Williams domain pattern in a few tenths of a second, while some hours are required to form a Williams domain pattern in T2/60. P-6 also differs from T2/60 in exhibiting a dynamic scattering mode. At threshold this pattern has a formation time of several seconds, which allows examination of its precursor pattern.

Introduction

Thermotropic nematic phases have been reported for a variety of polymers containing mesomorphic groups on the side chain or incorporated in the main chain. Recently, there has been increased interest in polymers having main-chain mesomorphism due to their potential application for the production of high-modulus fibers. These polymers may exhibit nematic, smectic, cholesteric, or twisted smectic mesophases or some combination of these in different temperature ranges. Identification of the type of mesophase is thus an important step in the characterization of these materials. Two of the more definitive procedures for characterization of low molecular weight mesogens, X-ray diffraction and mutual miscibility, have thus far not been widely applied to the characterization of polymeric mesophases. The presence of a nematic phase in a low molecular weight mesogen is often evidenced by the appearance, when viewed under the polarizing microscope, of "threads" in a birefringent fluid phase. Alternatively, the differential scanning calorimeter (DSC) can be used to distinguish between thermotropic nematic and smectic phases by the magnitude of the enthalpy change accompanying the transition to the isotropic phase. The interpretation of these same types of observation for polymeric mesophases is often less certain. A remnant of high-melting crystallites may produce what appears to be an anisotropic fluid phase,¹ and on occasion the threadlike pattern of disclinations forms with great reluctance (or not at all) in a highly viscous polymeric nematic phase. Also, the interpretation of DSC data for polymeric mesophases may be complicated by transitions involving different crystalline polymorphs and by a variable degree of supercooling, which appears to be characteristic of the isotropic-nematic transition in polymers. Further, the paucity of experimental data precludes a confident prediction of the magnitude of the enthalpy changes expected for transitions of the different types of mesophases in

polymers. These difficulties led to the exploration^{2,3} of electric field induced instabilities as a possible confirmatory test for the presence of a thermotropic nematic phase in polymers. The first investigations were performed with Tennessee Eastman T2/60, a poly(ethylene terephthalate-co-1,4-benzoate) containing 60 mol % *p*-oxybenzoyl units. Electrohydrodynamic instabilities observed in this polymeric nematic phase included the analogues of the Williams domain pattern,⁴ the variable grating mode,^{5,6} and high-field turbulence.⁷ These observations were compared^{2,3} with the corresponding instability patterns seen in *p*-azoxyanisole (PAA), the classical low molecular weight thermotropic nematogen. Analogues of the chevron pattern⁸ and the dynamic scattering mode (DSM)⁹ were not observed in this polymer.

These results gave promise that electric field effects might furnish a useful diagnostic tool for nematic phases in polymers. On the other hand, it was recognized² that additional work on a variety of polymers would be required to assess the generality of this procedure as a confirmatory test. In the present paper we report the results of a study of electric field effects using a polyester synthesized from 4,4'-dihydroxy- α -methylstilbene and adipic acid.^{10,11}



One of the disadvantages of the use of electrohydrodynamic effects for diagnostic purposes, as revealed by our earlier studies, is the long formation time on the instability patterns. For example, the formation time of Williams domain patterns in T2/60 was of the order of an hour, as compared to tenths to hundredths of a second in PAA. We presumed this difference was due to the high viscosity of the polymeric mesophase. If this explanation is correct, it should be possible to reduce the formation time by examining polymeric samples of low molecular weight. The